Acta Crystallographica Section C
Crystal Structure Communications
ISSN 0108-2701

2,3-Dihydro-1,3-benzothiazol-2-iminium monohydrogen sulfate and 2-iminio-2,3-dihydro-1,3-benzothiazole-6-sulfonate: a combined structural and theoretical study

Rafal Kruszynski* and Agata Trzesowska-Kruszynska

Institute of General and Ecological Chemistry, Technical University of Łódź, Zeromskiego 116, 90-924 Łódź, Poland
Correspondence e-mail: rafal.kruszynski@p.lodz.pl

Received 29 September 2009
Accepted 30 October 2009
Online 13 November 2009

The 2-aminobenzothiazole sulfonation intermediate 2,3-dihydro-1,3-benzothiazol-2-iminium monohydrogen sulfate, $C_7H_7N_2S^+\cdot HSO_4^-$, (I), and the final product 2-iminio-2,3-dihydro-1,3-benzothiazole-6-sulfonate, $C_7H_6N_2O_3S_2$, (II), both have the endocyclic N atom protonated; compound (I) exists as an ion pair and (II) forms a zwitterion. Intermolecular N—H···O and O—H···O hydrogen bonds are seen in both structures, with bonding energy (calculated on the basis of density functional theory) ranging from 1.06 to 14.15 kcal mol^{-1}. Hydrogen bonding in (I) and (II) creates *DDDD* and *C*(8)*C*(9)*C*(9) first-level graph sets, respectively. Face-to-face stacking interactions are observed in both (I) and (II), but they are extremely weak.

Comment

Benzothiazoles comprise a class of compounds that exhibit complex biological properties. Substituted benzothiazoles serve as selective antitumor agents (Akhtar *et al.*, 2008; Bradshaw *et al.*, 2002; Mortimer *et al.*, 2006), neurotransmission blockers (Jimonet *et al.*, 1999), and anti-infective and antifungal agents (Mittal *et al.*, 2007). In recent years, benzothiazoles have gained attention as part of the structure of the radical cation derived from 2,2′-azinobis-3-ethylbenzothiazoline-6-sulfonic acid, which is used for the evaluation of antioxidant efficiency (Osman *et al.*, 2006; Pellegrini *et al.*, 2003; Walker & Everette, 2009). Benzothiazoles have been recognized as therapeutically active skeletons that are useful for making fatty acid amide hydrolase inhibitors (Wang *et al.*, 2009). Sulfonated benzothiazoles represent a novel class of potent and selective antitrypanosomal agents (Tellez-Valencia *et al.*, 2002; Espinoza-Fonseca & Trujillo-Ferrara, 2005). Molecular docking simulations revealed that they form more energetically stable complexes with trypanosomal triosephosphate isomerase (TIM) than with human TIM, which is a crucial aspect for the design of new antiparasitic drugs, including those active against *Trypanosoma cruzi* which causes Chagas disease. The origin of the selectivity of these compounds has not yet been identified. It was postulated that bonding of the different drugs to the macromolecular species *via* noncovalent interactions has crucial importance (Szatyłowicz, 2008). In this context, the synthesis, structure and intermolecular interactions of new sulfonated 2-aminobenzothiazole derivatives are of interest. Hence, the solid-state characterization of the 2-aminobenzothiazole sulfonation intermediate and the final products, namely 2,3-dihydro-1,3-benzothiazol-2-iminium monohydrogen sulfate, (I), and 2-iminio-2,3-dihydro-1,3-benzothiazole-6-sulfonate, (II), as well as the results of quantum mechanical calculations, are reported here.

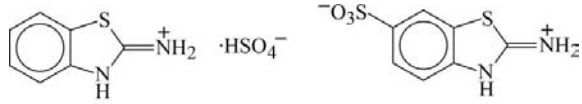

In both compounds, one of the acid group H atoms is transferred to the amine N atom of the 2-aminobenzothiazole molecule, so that the asymmetric unit of (I) consists of a 2,3-dihydro-1,3-benzothiazol-2-iminium ion and sulfuric acid in the monoionized state, *i.e.* monohydrogen sulfate (Fig. 1), and

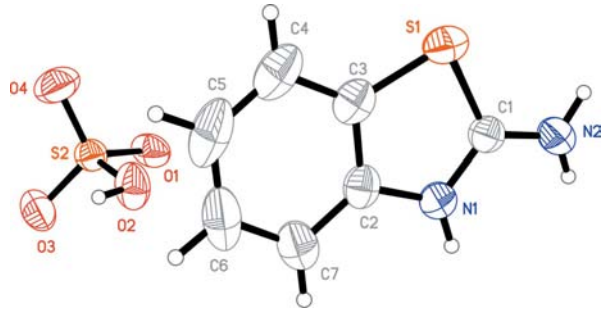

Figure 1
The molecular structure of (I). Displacement ellipsoids are drawn at the 50% probability level and H atoms are shown as spheres of arbitrary radii.

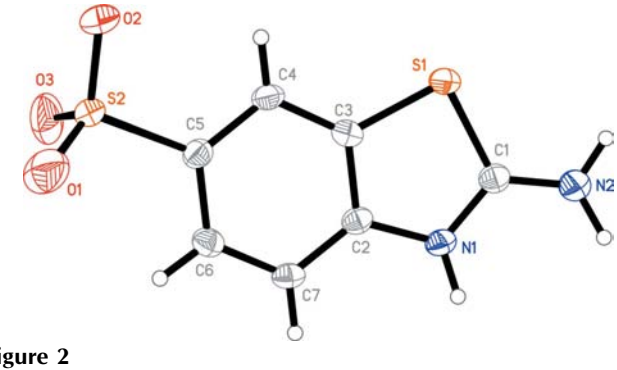

Figure 2
The molecular structure of (II). Displacement ellipsoids are drawn at the 50% probability level and H atoms are shown as spheres of arbitrary radii.

  doi:10.1107/S0108270109045673

compound (II) exists in the form of a zwitterion (Fig. 2). The 2,3-dihydro-1,3-benzothiazol-2-iminium cation is slightly distorted from planarity, the largest deviation from the weighted least-squares plane calculated through all non-H atoms of this cation being for atom N2 [0.0218 (13) Å in (I) and 0.0980 (13) Å in (II)]. The slightly larger deviation of atom N2 in (II) probably originates from an out-of-plane N2—H2*B*···O1^{vi} hydrogen bond [symmetry code: (vi) $-x$, $y-1$, $-z+\frac{1}{2}$], which may influence the position of atom N2 [in (I), the N2—H···O bonds are almost in the plane of the cation]. In (II), atom S2 lies 0.3235 (17) Å from the above-mentioned plane. Each of the five- and six-membered rings of the cation of (I) can be considered planar, and both ring systems are coplanar in the range of experimental error. The five- and six-membered rings of the molecule of (II) show some deviation from planarity [the most highly deviating atom from the five-membered ring being C1 and from the six-membered ring being C2, with deviations of 0.0184 (10) and 0.0195 (12) Å, respectively, from the ring weighted least-squares planes].

The bond distances and angles within the anion show no unusual values (Table 1). The bond lengths and angles of the 2,3-dihydro-1,3-benzothiazol-2-iminium cation (in both title compounds) are within the ranges reported for its adducts with organic anions (Lynch *et al.*, 1998, 1999; Smith *et al.*, 1999; Trzesowska-Kruszynska & Kruszynski, 2009) and are close to those of pure 2-aminobenzothiazole (ABT; Goubitz *et al.*, 2001). In comparison with ABT, the C2—N1, S1—C3 and C1—N2 bonds of (I) and (II) are shortened by an insignificant amount [by 0.017 (11), 0.024 (9) and 0.019 (12) Å, respectively, for (I), and by 0.009 (11), 0.011 (9) and 0.022 (12) Å, respectively, for (II)], while the C1—N1 bond is elongated by 0.052 (8) and 0.059 (8) Å, respectively, for (I) and (II). For similar 2-amino heterocyclic compounds, shortening of the C—NH_2 bond has been explained by the attraction of a more electron-accepting heterocyclic ring (Lynch & Jones, 2004). In both title compounds, the C1—N2 distance (Tables 1 and 2) is close to that of the exocyclic C=N double bonds found in iminobenzothiazole derivatives, *i.e.* to 1.312 (4) Å in {[1,3-benzothiazol-2(3*H*)-ylidene]amido}-*O*,*O*′-diethylphosphate sulfide (Garcia-Hernandez *et al.*, 2006), to 1.300 (3) Å in diethyl [(6-chloro-2,3-dihydrobenzothiazol-2-ylidene)amido]-thiophosphate (Shi *et al.*, 2003) and to 1.302 (4) Å in 1-(benzothiazol-2-ylidene)-3,3-dimethylthiourea (Tellez *et al.*, 2004). These observations point to a significant contribution of the exocyclic iminium resonance form, *i.e.* the 2,3-dihydro-1,3-benzothiazol-2-iminium ion and 2-iminio-2,3-dihydro-1,3-benzothiazole-6-sufonate, to the overall molecular electronic structures, with a lesser contribution from the 2-amino-benzothiazolium and 2-aminobenzothiazolium-6-sulfonate forms, respectively, for (I) and (II). Exocyclic imines or iminium ions in equilibrium with endocyclic imines have previously been found and discussed for other compounds containing the N_{exo}—C—N_{endo} group (Lynch & Jones, 2004; Lynch *et al.*, 2000; Low *et al.*, 2003; Donga *et al.*, 2002). The anion of (I) shows S—O distances typical for the HSO_4^- anion, with three almost equal shorter bonds lengths (Table 1) close to the mean value of 1.446 (2) Å obtained for 147 HSO_4^- ions existing in 115 structures and a longer S—OH bond almost equal to the mean value of 1.559 (1) Å obtained for 93 HSO_4^- ions existing in 74 structures (Allen, 2002) [the Kolmogorov–Smirnov test (Chakravarti, 1967) shows deviations from normal distribution and the skewness was 1.996, thus statistically asymmetric data of 41 structures were excluded from the calculation]. The S—O distances in the sulfonate group of (II) (Table 2) are also typical for ionized sulfonic acids.

The cations and anions of (I) are linked by N—H···O hydrogen bonds (Table 3) to form a hydrogen-bonded ribbon extending along the [010] axis (Fig. 3) and comprising N_1DDDD and $N_2C_2^1(4)C_2^2(6)C_2^2(8)C_2^2(8)[R_1^2(4)R_2^2(8)]$ basic graph sets (Bernstein *et al.*, 1995). The anions of (I) are connected *via* O—H···O hydrogen bonds (Table 3) to form a hydrogen-bonded chain propagating along the [001] axis and comprising $N_1C(4)$ motifs. These two types of interactions join ions of (I) to form a two-dimensional net parallel to the (100) plane. The zwitterions of (II) are connected by N—H···O hydrogen bonds (Fig. 4) to form a bilayer extending along the $(10\bar{1})$ plane and comprising patterns described by an $N_1C(8)C(9)C(9)$ basic graph set. An interesting feature of the structures of (I) and (II) is the presence of stacking interactions (along the [001] axis) between the almost parallel (Table 4) five-membered heterocyclic and benzene rings of adjacent amines. These stacking interactions provide some linkage within the hydrogen-bonded two-dimensional net of (I) and between the hydrogen-bonded sheets of (II). Moreover, there is a short intramolecular C—H···O contact in the structure of (II) which, according to Desiraju & Steiner (1999), can be classified as a weak hydrogen bond (Table 3).

The molecular electronic properties of (I) and (II) have been calculated at a single point for both diffraction-derived coordinates and the optimized structures. The structural

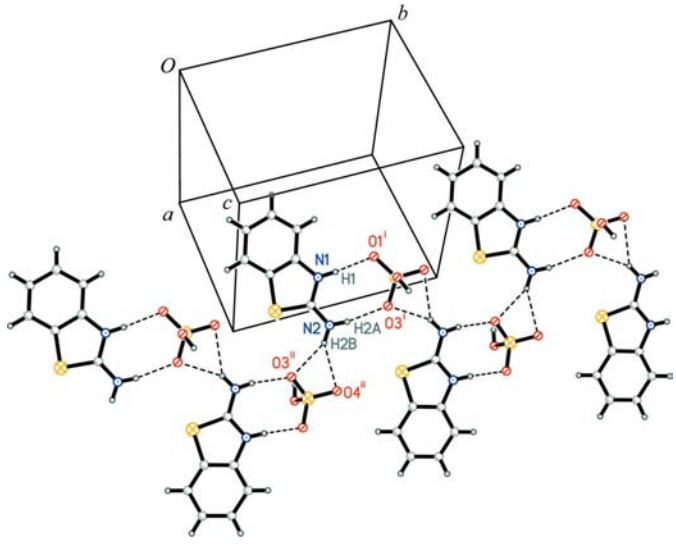

Figure 3
Part of the packing of molecules in (I), showing the hydrogen-bonded ribbon extending along the [010] axis. Dashed lines indicate N—H···O hydrogen bonds. [Symmetry codes: (i) $-x+1$, $-y+1$, $-z+2$; (ii) $x+1$, $-y+\frac{1}{2}$, $z+\frac{1}{2}$.]

parameters were used as the starting model in each calculation. Sets containing from one to five cation–anion pairs were used for the calculations for (I). The cation and anion of each pair were arranged in hydrogen-bonded sheets (three pairs) and in stacking interactions (next two pairs). The electrostatic interaction energies between anions and cations were estimated using the counterpoise method (Boys & Bernardi, 1970); for this purpose, additional computations were made in which the counterpoise method subsets contained odd numbers of cations and anions. For (II), the sets contained from two to seven zwitterions, and molecules were added one by one to the hydrogen-bond donors and acceptors of the starting molecule. The atomic and molecular properties were calculated at 298.15 K. The optimized geometrical parameters were in good agreement with those found from X-ray measurements, although geometrically optimized molecules show a typical elongation of the C—H, N—H and O—H bonds (from 0.03 to 0.19 Å). This effect leads to a slight narrowing of the D—H$\cdots A$ angles, but the $D\cdots A$ distances remain unchanged. The B3LYP functional (Becke, 1993; Lee *et al.*, 1988) in the triple-ζ 6–31++G(3*df*,2*p*) basis set was used, as implemented in *GAUSSIAN03* (Frisch *et al.*, 2004). The differences in electronic properties and energies originating from the different numbers of molecules used in the calculations are given in parentheses in the *Comment* and in Table 3 as standard deviations of the arithmetic mean values. Where no deviation is given, the values were the same within the range of reported precision. The atomic charges were calculated according to the natural population analysis (NPA; Foster & Weinhold, 1980; Reed & Weinhold, 1985; Reed *et al.*, 1988), Merz–Kollman–Singh (MKS; Singh & Kollman, 1984; Besler *et al.*, 1990) and Breneman (Breneman & Wiberg, 1990) schemes. Although the calculation of effective atomic charges plays an important role in the application of quantum mechanical calculations to molecular systems, the unambiguous division of the overall molecular charge density into atomic contributions is still an unresolved problem, and none of the known procedures give completely reliable values of atomic charges. Thus, a discussion of atomic charges should cover more than one algorithm used for charge density division. Generally, it can be stated that less reliable values are given by the Mulliken population analysis and more reliable results are provided by the Breneman method [for a detailed discussion of the methodology and reliability of the methods used, see Martin & Zipse (2005), and references therein].

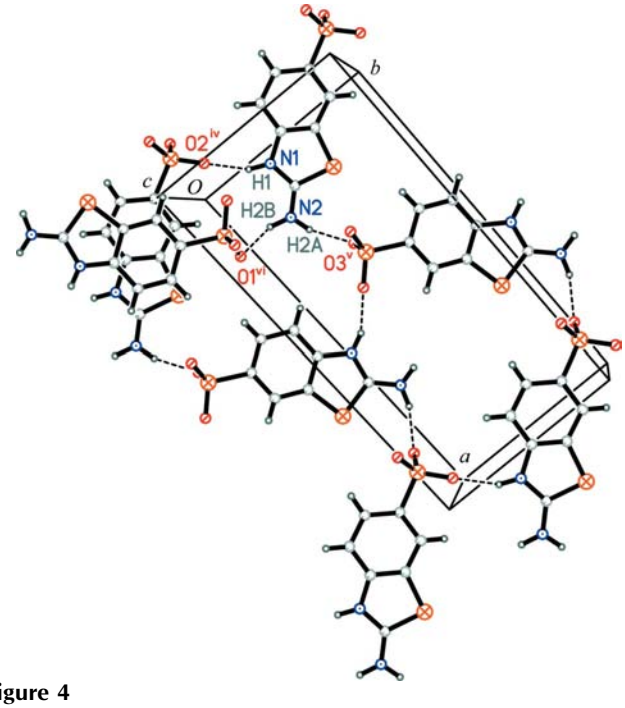

Figure 4
Part of the packing of molecules in (II), showing N—H$\cdots$O hydrogen bonds (as dashed lines). [Symmetry codes: (iv) $x, y-1, z$; (v) $x+\frac{1}{2}, -y+\frac{3}{2}, z+\frac{1}{2}$; (vi) $-x, y-1, -z+\frac{1}{2}$.]

In general, all N—H$\cdots$O and O—H$\cdots$O hydrogen bonds in (I) and (II) can be considered as medium strength or weak intermolecular bonding interactions. The second-order perturbation theory analysis of the Fock matrix in the natural bond orbital (NBO) basis leads to the conclusion that N—H$\cdots$O interactions are formed mostly by hydrogen-bond-acceptor lone pairs donating electron density to the antibonding orbitals of D—H bonds, and these 'delocalization' energies [$E_{\mathrm{del}(1)}$] are collected in Table 3. The second most energetic interactions [$E_{\mathrm{del}(2)}$] have the same contributions of atomic orbitals; however, the other lone pairs of the O atoms are used. The $E_{\mathrm{del}(2)}$ values are distinctly lower than $E_{\mathrm{del}(1)}$ in all cases [for example, for N1—H1$\cdots$O1$^{\mathrm{i}}$, $E_{\mathrm{del}(2)}$ = 3.28 kcal mol^{-1}; symmetry code: (i) $-x+1, -y+1, -z+2$]. The following weaker interactions are multiple interactions between acceptor lone pairs and one-centre Rydberg antibonding orbitals of H atoms. These results are in opposition to previous findings for ether and nitric group O atoms acting as donors of hydrogen bonds (Kruszynski, 2008, 2009), where $E_{\mathrm{del}(2)}$ interactions were related to one-centre Rydberg antibonding orbitals of hydrogen-bond donors. This can be explained by the different character of O atoms in monoionized sulfate or sulfonate compared with that in uncharged groups that form part of organic molecules. The localization of negative charge on the O atoms in (I) and (II) leads to the formation of an additional electron lone pair, which is able to donate its internal electron density to other species. On the basis of the geometrical parameters, the intramolecular C4—H4$\cdots$O2 interaction can be regarded as a weak hydrogen bond; however, the very low energy of this interaction (Table 3) suggests that it originates from an accidental molecular arrangement (enforced by other geometric and energetic factors). The stacking interactions are formed by bonding π orbitals of one ring donating electron density to the antibonding π orbitals of the second ring and to one-centre Rydberg antibonding orbitals of π-bonded atoms of the rings. These interactions are extremely weak (Table 4) but they are still bonding in character. The energies of intermolecular interactions, calculated on the basis of total self-consistent field energy [E_{SCF}, corrected for basis-set superposition error estimated by use of the counterpoise method (Boys & Bernardi, 1970)], are very close to the respective NBO total energies (E, Tables 3 and 4) or their sums [N1—H1$\cdots$O1$^{\mathrm{i}}$ +

N2—H2A···O3^{i} and N2—H2B···O3^{ii} + N2—H2B···O4^{ii}; symmetry code: (ii) $x+1, -y+\frac{1}{2}, z+\frac{1}{2}$]. The differences are not larger than 0.48 kcal mol^{-1} for N—H···O and O—H···O hydrogen bonds, and 0.02 kcal mol^{-1} for C—H···O and each π–π interaction. In all cases, the E_{SCF} values are slightly larger than those obtained on the NBO basis. For N—H···O and O—H···O hydrogen bonds this difference is caused by bonding σ orbitals of the acceptor donating electron density to the one-centre Rydberg antibonding orbitals of the donor H atoms, and for other interactions the above-mentioned enlargement originates from contributions of acceptor occupied orbitals other than those of the lone pairs (*e.g.* one-centre Rydberg antibonding orbitals). In general, the strength of the N—H···O and O—H···O interactions does not correlate directly with the enlargement of the D···A distance or D—H···A angle, but a general relationship of increasing hydrogen-bond energy with both decreasing D···A distance and increasing D—H···A angle is observed (Fig. 5). As expected, in (I) there is a large attractive electrostatic interaction between ions of the opposite charge; this is equal to about 62.9 and 70.6 kcal mol^{-1}, respectively, for cations and anions connected by N1—H1···O1^{i} and N2—H2B···O3^{ii} intermolecular interactions. The repulsive force between neighbouring anions is about 31.17 kcal mol^{-1} and that between neighbouring cations is about 55.4 kcal mol^{-1}. Quantum-mechanical study of the electronic structure of the C—N bonds shows the same behaviours as previously described for 2,3-dihydro-1,3-benzothiazol-2-iminium hydrogen oxydiacetate (Trzesowska-Kruszynska & Kruszynski, 2009), which confirms that electron density is localized in the exocyclic rather than the endocyclic C—N bond and, in consequence, that the exocyclic iminium resonance form is predominant.

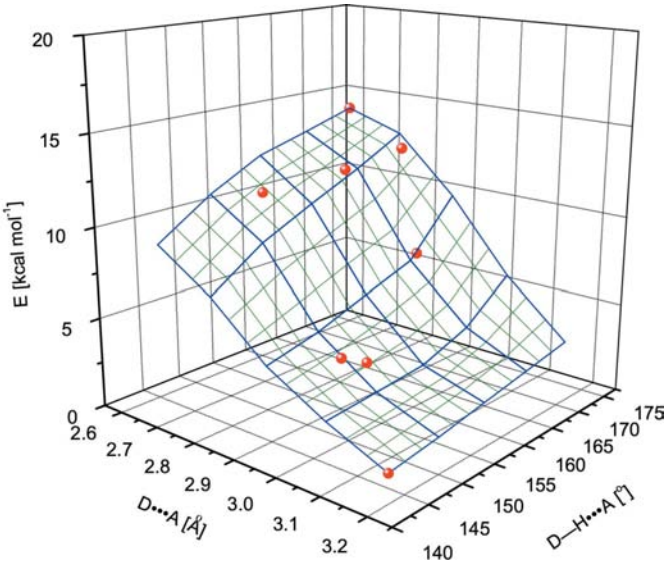

Figure 5
A surface plot showing the relationship between hydrogen-bond energy (E, Table 3) and D···A distances/D—H···A angles. The values of E for (I) and (II) are indicated by dots.

Analysis of the NPA and MKS charges and those derived from electrostatic properties using the Breneman radii shows that, in general, the atomic charges do not depend on the method used for calculation. In both compounds, all N atoms are negatively charged [the N1 atoms slightly less than the N2 atoms; charges are, respectively, −0.46 (3) and −0.69 (7) a.u. for (I), and −0.50 (6) and −0.68 (6) a.u. for (II), where a.u. denotes the atomic unit, equal to the charge of one electron], but the NH group of the thiazole ring has a negative group charge [−0.19 (2) and −0.20 (1) a.u., respectively, for (I) and (II)], whereas the NH_2 group has a positive group charge [0.21 (2) and 0.18 (1) a.u., respectively, for (I) and (II)]. Such a distribution of charges is observed only in the 2,3-dihydro-1,3-benzothiazol-2-iminium ion, so these calculated values confirm again the postulated dominance of the exocyclic iminium resonance form. The O atoms of the monohydrogen sulfate and sulfonate group are negatively charged but a difference of about 0.1 a.u. is observed between the O atom of the hydroxy group [possessing a −0.90 (3) a.u. charge] and the other O atoms of (I) and (II) [having charges from −1.00 (4) to −1.06 (3) a.u.]. It is noteworthy that in the case of calculations performed for separated (non-interacting) ions or molecules the positive charges on H atoms [0.18 (3)–0.43 (1) a.u.] involved in hydrogen bonds are about 0.03 a.u. larger, and negative charges on hydrogen-bond-acceptor O atoms are about 0.02 a.u. smaller than those in interacting molecules. This confirms that during the formation of an intermolecular interaction a transfer of electron density occurs.

Experimental

Commercially available 2-aminobenzothiazole (0.05 mol, 7.5099 g) was dissolved in 96% sulfuric acid (2.8 ml, 0.05 mol), and water (2.0 ml) was added dropwise over a period of 10 min to avoid overheating. The solution was stored at 283.2 (3) K for 14 h, during which time a crystalline product was formed. The crystals of (I) were filtered off using a Buchner filter funnel with integral sintered glass disc (G3 type) placed in an ice cooling jacket. The product was dried in a vacuum desiccator (at a pressure of 200 Pa) for 6 h (yield 83%). The crystal for measurement was selected directly from the dry sample.

Commercially available 2-aminobenzothiazole (0.02 mol, 3.0040 g) was dissolved in 96% sulfuric acid (10.0 ml, 0.18 mol). The mixture was heated [at 433 (1) K] under reflux for 35 min, cooled to room temperature and poured into cold water. Compound (II), which is insoluble in water, precipitated at the bottom of the beaker, was washed with water (7 ml) three times by decantation and was transferred quantitatively to a Buchner filter funnel with integral sintered glass disc (G5 type). The product was washed with water (5 × 10 ml) and dried in a vacuum desiccator (at a pressure of 200 Pa) for 9 h (yield 98.7%). Crystals suitable for measurement were obtained by dissolving (II) (2.3026 g) in 96% sulfuric acid (4 ml) and adding small portions of water (0.02 ml) every 10 min for 8 d. The obtained crystals were filtered off using a Buchner filter funnel with integral sintered glass disc (G5 type), washed with water (5 × 5 ml) and dried in a vacuum desiccator (at a pressure of 200 Pa) for 14 h. Compound (II) can be also obtained by moistening of pulverized (I) (2.4827 g, 0.01 mol) with 96% sulfuric acid (0.3 ml) and heating of the sample at 403 K for 1 h [(I) is converted to (II) in stochiometric quantity].

Vibrational analysis was carried out for both compounds. The IR spectra (400–4000 cm^{-1}) were recorded as KBr discs in a Bruker spectrophotometer. The IR spectra of (I) and (II) contain characteristic bands of stretching vibrations of the NH_2, NH and CH groups in the region of 3600–3000 cm^{-1}. The single band at 1645 cm^{-1} is attributed to the CN stretching vibrations and NH bending vibrations. The bands around 1600, 1580 and 1470 cm^{-1} confirm the presence of aromatic C—C bonds. The medium intensity bands at 750 cm^{-1} in (I) and 840 cm^{-1} in (II) correspond to vibrations of aryl CH bonds. An important spectral feature that can be used to distinguish the hydrogen sulfate and sulfonate ions is the CS stretching vibration, which typically occurs at 1140 and 735 cm^{-1}. The bands corresponding to this vibration appear at 1143 and 731 cm^{-1} only in the IR spectrum of compound (II). The broad split absorption bands in the frequency range 1170–1210 cm^{-1} are attributed to the asymmetric S═O vibrations of the sulfate [in (I)] and sulfonate [in (II)] groups. The broadening is caused by the presence of noncovalent interactions in the solid state. The symmetric S═O vibrations appear as strong bands at 1005 cm^{-1} for (I) and 1028 cm^{-1} for (II). Additionally, the IR spectrum of (I) showed a medium intensity band at 1067 cm^{-1} originating from stretching vibrations of OH bonds from the HSO_4^- anion, whereas the broad band in the frequency range 850–883 cm^{-1} can be attributed to vibrations of S—OH groups.

Compound (I)

Crystal data

$C_7H_7N_2S^+\cdot HSO_4^-$
M_r = 248.27
Monoclinic, $P2_1/c$
a = 11.1693 (4) Å
b = 10.2261 (3) Å
c = 9.0551 (3) Å
β = 102.799 (3)°
V = 1008.56 (6) Å^3
Z = 4
Mo $K\alpha$ radiation
μ = 0.52 mm^{-1}
T = 291 K
0.31 × 0.15 × 0.12 mm

Data collection

Kuma KM-4 CCD diffractometer
Absorption correction: numerical (*X-RED*; Stoe & Cie, 1999)
T_{min} = 0.908, T_{max} = 0.941
9680 measured reflections
1797 independent reflections
1603 reflections with $I > 2\sigma(I)$
R_{int} = 0.023

Refinement

$R[F^2 > 2\sigma(F^2)]$ = 0.031
$wR(F^2)$ = 0.090
S = 1.06
1797 reflections
136 parameters
H-atom parameters constrained
$\Delta\rho_{max}$ = 0.26 e Å^{-3}
$\Delta\rho_{min}$ = −0.44 e Å^{-3}

Table 1
Selected bond lengths (Å) for (I).

N1—C1	1.330 (2)	S2—O4	1.4216 (16)
N1—C2	1.388 (2)	S2—O3	1.4447 (14)
C1—N2	1.315 (2)	S2—O1	1.4616 (13)
C1—S1	1.722 (2)	S2—O2	1.5546 (15)
S1—C3	1.747 (2)		

Table 2
Selected bond lengths (Å) for (II).

N1—C1	1.337 (3)	C5—S2	1.776 (2)
N1—C2	1.396 (2)	S2—O2	1.4454 (18)
C1—N2	1.312 (3)	S2—O1	1.4503 (18)
C1—S1	1.747 (2)	S2—O3	1.4628 (18)
S1—C3	1.7604 (19)		

Table 3
Experimental hydrogen-bond geometry (Å, °), total energy E (kcal mol^{-1}) and principal 'delocalization' energy $E_{del(1)}$ calculated on the NBO basis for (I) and (II) with the standard deviations (for details of standard deviation calculation, see *Comment*) (1 kcal mol^{-1} = 4.184 kJ mol^{-1}).

D—H···A	D—H	H···A	D···A	D—H···A	E	$E_{del(1)}$
(I)						
N1—H1···O1^{i}	0.86	1.94	2.792 (2)	171.8	12.43 (2)	6.30 (1)
N2—H2A···O3^{i}	0.84	2.05	2.873 (3)	169.1	6.83 (1)	3.62
N2—H2B···O3^{ii}	0.86	2.21	2.995 (2)	153.1	3.69	2.87
N2—H2B···O4^{ii}	0.86	2.45	3.180 (2)	144.2	1.06	0.90
O2—H2C···O1^{iii}	0.85	1.79	2.6296 (18)	173.1	14.15 (2)	6.64 (1)
(II)						
N1—H1···O2^{iv}	0.91	1.84	2.690 (2)	155.7	10.96 (1)	8.55 (1)
N2—H2A···O3^{v}	0.90	1.90	2.774 (2)	163.5	11.87 (2)	5.56
N2—H2B···O1^{vi}	0.95	2.16	3.013 (3)	148.2	4.87	2.69
C4—H4···O2	0.93	2.55	2.895 (3)	102.4	0.11	0.07

Symmetry codes: (i) $-x+1, -y+1, -z+2$; (ii) $x+1, -y+1/2, z+\frac{1}{2}$; (iii) $x, -y+\frac{1}{2}, z-\frac{1}{2}$; (iv) $x, y-1, z$; (v) $x+\frac{1}{2}, -y+\frac{3}{2}, z+\frac{1}{2}$; (vi) $-x, y-1, -z+\frac{1}{2}$.

Compound (II)

Crystal data

$C_7H_6N_2O_3S_2$
M_r = 230.26
Monoclinic, $C2/c$
a = 18.9085 (11) Å
b = 8.2360 (6) Å
c = 12.9684 (10) Å
β = 121.605 (9)°
V = 1720.0 (2) Å^3
Z = 8
Mo $K\alpha$ radiation
μ = 0.60 mm^{-1}
T = 291 K
0.28 × 0.28 × 0.26 mm

Data collection

Kuma KM-4 CCD diffractometer
Absorption correction: numerical (*X-RED*; Stoe & Cie, 1999)
T_{min} = 0.847, T_{max} = 0.860
8399 measured reflections
1531 independent reflections
1497 reflections with $I > 2\sigma(I)$
R_{int} = 0.050

Refinement

$R[F^2 > 2\sigma(F^2)]$ = 0.034
$wR(F^2)$ = 0.089
S = 1.08
1531 reflections
127 parameters
H-atom parameters constrained
$\Delta\rho_{max}$ = 0.28 e Å^{-3}
$\Delta\rho_{min}$ = −0.53 e Å^{-3}

C-bonded H atoms were placed in calculated positions (C—H = 0.93 Å) and refined as part of a riding model, with U_{iso}(H) = 1.2U_{eq}(C). Other H atoms were found from difference Fourier syntheses and after eight cycles of anisotropic refinement they were incorporated directly into a riding model, with U_{iso}(H) = 1.2U_{eq}(N) and 1.5U_{eq}(O). Further details of the refinements are available in the archived CIF.

For both compounds, data collection: *CrysAlis CCD* (UNIL IC & Kuma, 2000); cell refinement: *CrysAlis RED* (UNIL IC & Kuma, 2000); data reduction: *CrysAlis RED*; program(s) used to solve structure: *SHELXS97* (Sheldrick, 2008); program(s) used to refine structure: *SHELXL97* (Sheldrick, 2008); molecular graphics: *XP* in *SHELXTL/PC* (Sheldrick, 2008) and *ORTEP-3* (Farrugia, 1997); software used to prepare material for publication: *SHELXL97* and *PLATON* (Spek, 2009).

This work was financed by funds allocated by the Ministry of Science and Higher Education to the Institute of General and Ecological Chemistry, Technical University of Lodz,

Table 4
Experimental stacking interactions geometry (Å, °), total energy E (kcal mol^{-1}) and principal 'delocalization' energy $E_{del(1)}$ calculated on the NBO basis for (I) and (II).

$CgJ\cdots CgK$	$Cg\cdots Cg$	α	β	CgJ_{perp}	E	$E_{del(1)}$
(I)						
$Cg5\cdots Cg6^{vii}$	3.5898	0.90	13.16	3.488	0.16	0.04
$Cg6\cdots Cg5^{iii}$	3.5898	0.90	13.68	3.495	0.16	0.04
(II)						
$Cg5\cdots Cg6^{viii}$	3.5684	7.72	17.96	3.222	0.17	0.04
$Cg6\cdots Cg5^{viii}$	3.5684	7.72	25.46	3.395	0.17	0.04
$Cg6\cdots Cg6^{viii}$	3.5642	3.47	19.05	3.369	0.17	0.03
$Cg5\cdots Cg6^{ix}$	3.6140	4.43	22.22	3.264	0.16	0.02
$Cg6\cdots Cg5^{ix}$	3.6140	4.43	25.41	3.345	0.16	0.02

Notes: $Cg5$ and $Cg6$ are the ring centroids of the five- and six-membered rings, respectively, $Cg\cdots Cg$ is the perpendicular distance between the first ring centroid and that of the second ring, α is the dihedral angle between planes J and K, β is the angle between the vector linking the ring centroid and the normal to the ring J, and CgJ_{perp} is the perpendicular distance of the J ring centroid on ring K. Symmetry codes: (iii) $x, -y+\frac{1}{2}, z-\frac{1}{2}$; (vii) $x, -y+\frac{1}{2}, z+\frac{1}{2}$; (viii) $-x, y, -z+\frac{1}{2}$; (ix) $-x, -y+1, -z$.

under grant No. I-17/BW/74/08. The *GAUSSIAN03* calculations were carried out at the Academic Computer Centre ACK CYFRONET of the University of Science and Technology (AGH) in Cracow, Poland, under grant No. MNiSW/SGI3700/PŁódzka/040/2008.

Supplementary data for this paper are available from the IUCr electronic archives (Reference: UK3015). Services for accessing these data are described at the back of the journal.

References

Akhtar, T., Hameed, S., Al-Masoudi, N. A., Loddo, R. & La Colla, P. (2008). *Acta Pharm.* **58**, 135–149.
Allen, F. H. (2002). *Acta Cryst.* B**58**, 380–388.
Becke, A. D. (1993). *J. Chem. Phys.* **98**, 5648–5652.
Bernstein, J., Davis, R. E., Shimoni, L. & Chang, N.-L. (1995). *Angew. Chem. Int. Ed. Engl.* **34**, 1555–1573.
Besler, B. H., Merz, K. M. Jr & Kollman, P. A. (1990). *J. Comput. Chem.* **11**, 431–439.
Boys, S. F. & Bernardi, F. (1970). *Mol. Phys.* **19**, 553–566.
Bradshaw, T. D., Bibby, M. C., Double, J. A., Fichtner, I., Cooper, P. A., Alley, M. C., Donohue, S., Stinson, S. F., Tomaszewjski, J. E., Sausville, E. A. & Stevens, M. F. G. (2002). *Mol. Cancer Ther.* **1**, 239–246.
Breneman, C. M. & Wiberg, K. B. (1990). *J. Comput. Chem.* **11**, 361–373.
Chakravarti, I. M., Laha, R. G. & Roy, J. (1967). *Handbook of Methods of Applied Statistics*, Vol. I, pp. 392–394. New York: John Wiley and Sons.
Desiraju, G. R. & Steiner, T. (1999). *The Weak Hydrogen Bond in Structural Chemistry and Biology*, IUCr Monograph on Crystallography 9. Oxford University Press.
Donga, H.-S., Quan, B. & Tian, H.-Q. (2002). *J. Mol. Struct.* **641**, 147–152.
Espinoza-Fonseca, L. M. & Trujillo-Ferrara, J. G. (2005). *Biochem. Biophys. Res. Commun.* **328**, 922–928.
Farrugia, L. J. (1997). *J. Appl. Cryst.* **30**, 565.
Foster, J. P. & Weinhold, F. A. (1980). *J. Am. Chem. Soc.* **102**, 7211–7218.
Frisch, M. J., *et al.* (2004). *GAUSSIAN03.* Revision C.02. Gaussian Inc., Wallingford, CT, USA.
Garcia-Hernandez, Z., Flores-Parra, A., Grevy, J. M., Ramos-Organillo, A. & Contreras, R. (2006). *Polyhedron*, **25**, 1662–1672.
Goubitz, K., Sonneveld, E. J. & Schenk, H. (2001). *Z. Kristallogr.* **216**, 176–181.
Jimonet, P., *et al.* (1999). *J. Med. Chem.* **42**, 2828–2843.
Kruszynski, R. (2008). *Cent. Eur. J. Chem.* **6**, 542–548.
Kruszynski, R. (2009). *Acta Cryst.* C**65**, o396–o399.
Lee, C., Yang, W. & Parr, R. G. (1988). *Phys. Rev. B*, **37**, 785–789.
Low, J. N., Cobo, J., Abonia, R., Insuasty, B. & Glidewell, C. (2003). *Acta Cryst.* C**59**, o669–o671.
Lynch, D. E., Daly, D. & Parsons, S. (2000). *Acta Cryst.* C**56**, 1478–1479.
Lynch, D. E. & Jones, G. D. (2004). *Acta Cryst.* B**60**, 748–754.
Lynch, D. E., Nicholls, L. J., Smith, G., Byriel, K. A. & Kennard, C. H. L. (1999). *Acta Cryst.* B**55**, 758–766.
Lynch, D. E., Smith, G., Byriel, K. A. & Kennard, C. H. L. (1998). *Aust. J. Chem.* **51**, 587–592.
Martin, F. & Zipse, H. J. (2005). *Comput. Chem.* **26**, 97–105.
Mittal, S., Samota, M. K., Kaur, J. & Seth, G. (2007). *Phosphorus Sulfur Silicon Relat. Elem.* **182**, 2105–2113.
Mortimer, C. G., Wells, G., Crochard, J. P., Stone, E., Bradshaw, T. D., Stevens, M. F. G. & Westwell, A. D. (2006). *J. Med. Chem.* **49**, 179–185.
Osman, A. M., Wong, K. K. Y. & Fernyhough, A. (2006). *Biochem. Biophys. Res. Commun.* **346**, 321–329.
Pellegrini, N., Del Rio, D., Colombi, B., Bianchi, M. & Brighenti, F. (2003). *J. Agric. Food Chem.* **51**, 260–264.
Reed, A. E., Curtis, L. A. & Weinhold, F. A. (1988). *Chem. Rev.* **88**, 899–926.
Reed, A. E. & Weinhold, F. A. (1985). *J. Chem. Phys.* **83**, 1736–1740.
Sheldrick, G. M. (2008). *Acta Cryst.* A**64**, 112–122.
Shi, B., Chen, R. & Huang, Y. (2003). *Acta Cryst.* E**59**, o870–o872.
Singh, U. C. & Kollman, P. A. (1984). *J. Comput. Chem.* **5**, 129–145.
Smith, G., Cooper, C. J., Chauhan, V., Lynch, D. E., Healy, P. & Parsons, S. (1999). *Aust. J. Chem.* **52**, 695–704.
Spek, A. L. (2009). *Acta Cryst.* D**65**, 148–155.
Stoe & Cie (1999). *X-RED*. Version 1.18. Stoe & Cie GmbH, Darmstadt, Germany.
Szatyłowicz, H. (2008). *J. Phys. Org. Chem.* **21**, 897–914.
Tellez, F., Cruz, A., Lopez-Sandoval, H., Ramos-Garcia, I., Gayosso, M., Castillo-Sierra, R. N., Paz-Michel, B., Noth, H., Flores-Parra, A. & Contreras, R. (2004). *Eur. J. Org. Chem.* pp. 4203–4214.
Tellez-Valencia, A., Avila-Rios, S., Perez-Montfort, R., Rodriguez-Romero, A., de Gomez-Puyou, M. T., Lopez-Calahorra, F. & Gomez-Puyou, A. (2002). *Biochem. Biophys. Res. Commun.* **295**, 958–963.
Trzesowska-Kruszynska, A. & Kruszynski, R. (2009). *Acta Cryst.* C**65**, o19–o23.
UNIL IC & Kuma (2000). *CrysAlis CCD* and *CrysAlis RED*. Versions 1.163. Kuma Diffraction Instruments GmbH, Wrocław, Poland.
Walker, R. B. & Everette, J. D. (2009). *J. Agric. Food Chem.* **57**, 1156–1161.
Wang, X., Sarris, K., Kage, K., Zhang, D., Brown, S. P., Kolasa, T., Surowy, C., El Kouhen, O. F., Muchmore, S. W., Brioni, J. D. & Stewart, A. O. (2009). *J. Med. Chem.* **52**, 170–180.